Chapter 11

High Sensitive Piezoresistive Cantilever MEMS Based Sensor by Introducing Stress Concentration Region (SCR)

Sh Mohd Firdaus, Husna Omar and Ishak Abd Azid

Additional information is available at the end of the chapter

http://dx.doi.org/10.5772/48426

1. Introduction

Micro-Electromechanical System (MEMS) device has become a hallmark technology for the 21st century. Its capability to sense, analyse, compute and control all within a single chip provide many new and powerful products. MEMS device is an emerging device in several areas of science and technology such as engineering structure, electronics and life sciences field such as chemistry, physic, biology and health sciences [Chollet and Liu (2007), Chivukula et al. (2006), Madou (1997)]. The two main key features for MEMS based device are mechanical structure that can be equated to motion and electrical signal. The addition of mechanical structure to an electronic chip gives a great enhancement to the functionality and performance. These devices have been dominantly used in the current market for computer storage system and automobiles [Madou (1997), Beeby et al. (2004), Hsu (2002)]. Smart vehicle are based on the extensive use of sensors and actuators. Various kind of sensors are used to detect the environment or road conditions and the actuators are used to execute any action are required to deals with conditions happen such as accelerometer for airbag system and Global positioning System (GPS) [Madou (1997), Hsu (2002)]. Most MEMS device are basically base on mechanical structure like cantilever beam, gears, pump and motor as shown in Fig. 1.

2. MEMS and finite element analysis

MEMS devices deal with nanofabrication process which related to microelectronics fabrication technology. This fabrication involves a series of high tech and high cost process such as ultraviolet lithography and doping. Due to expensive cost of fabrication, finite element analysis (FEA) has been used to characterize the MEMS structure behaviour during

DNA binding, through a water flow and vibration testing [Chollet and Liu (2007), Chivukula et al. (2006)]. FEA software helps MEMS designers to identify potential problem at early stage in design cycle before proceed on fabrication or production line, its help reducing working time to market. In design cycle, MEMS devices need to be check design intent, working operation, collision avoidance/detection and package stack-up. FEA capability scaling down from sub-micron to angstroms level features help designers come up with lower scale device design towards lead nano sensor/ actuator. Some MEMS base sensor devices is an assemblies of several parts and packaging, by using FEA, collision and contact surface can be determine [Hsu (2002), Liu (2006)].

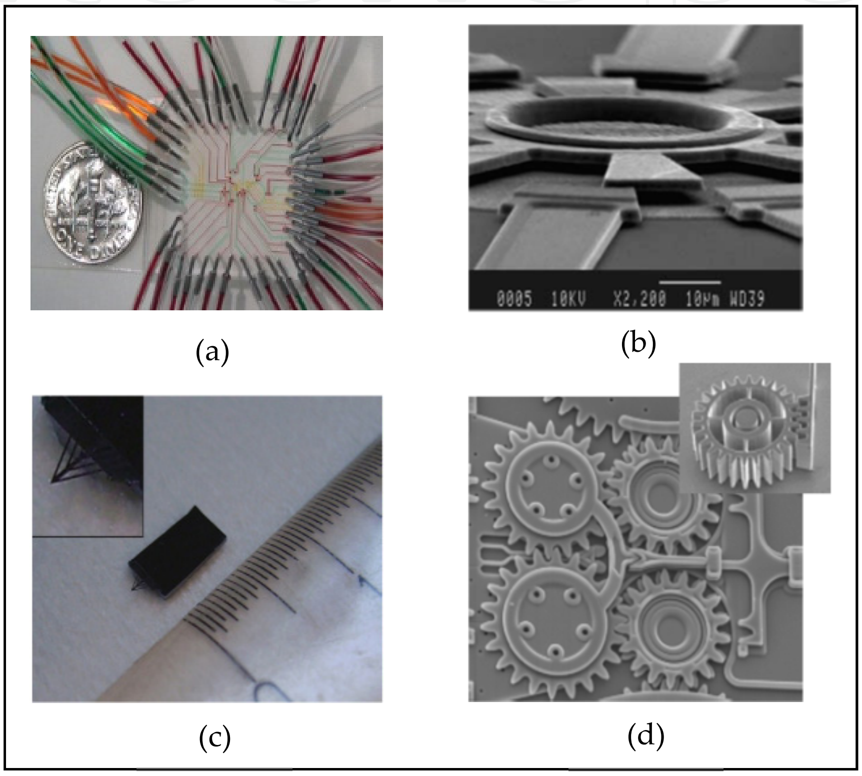

Figure 1. Example of MEMS devices; (a) micropump, (b) micromotor, (c) microcantilever, (d) microgears [Madou (1997), Hsu (2002), Arik et al. (1999)]

There are many FE software available in the market that has been used for analyse MEMS device like ANSYS, Solidworks, and Abaqus etc. Besides that there are also special dedicated MEMS FE software that integrates with MEMS device fabrication process such as CoventorWare, and IntelliCAD. In both software the modelling and fabrication file were combined and can transferred the fabrication machine [Madou (1997)]. The fabrication will be based on the attachment or design modelling file. This will not only help the MEMS designers to analyse and optimize the MEMS device design but also the manufacturability of the designed device. Flexibility in creating multiple design variations covering a wide range of needs such as die-mounted, package assemblies up to device efficiencies of configurations lead researchers to develop new device without any fabrication or prototype cost [Madou (1997), Hsu (2002), Liu (2006)].

3. Cantilever MEMS based sensor and finite element analysis

Brugger et al. (1999) and Thundat et al. (1995) have pointed out that cantilever based sensors are the simplest devices among MEMS devices that offer a very promising future for the development of novel physical, chemical and biological sensors. They have also been proven to be very versatile devices and have been used in several fields such as accelerometer, chemical sensors, etc [Vashist (2007)].

Basically MEMS cantilever sensor relies on the mechanical deformation of the structure, or in other words the deflection of membrane or beam structure. When the cantilever is loaded, its stressed elements deform. The MEMS cantilever will bend. As this deformation occur, the structure changes shape, and points on the structure displace. The concept is that deflection occurs when a disturbance or loading is applied to the cantilever is free end or along the MEMS cantilever surface. Normally the disturbance or loading is a force or mass that is attached to the MEMS cantilever in which it will make the MEMS cantilever bending Fig. 2 illustrates MEMS cantilever deflection working principal [Madou (1997), Hsu (2002), Lee et al. (2007)].

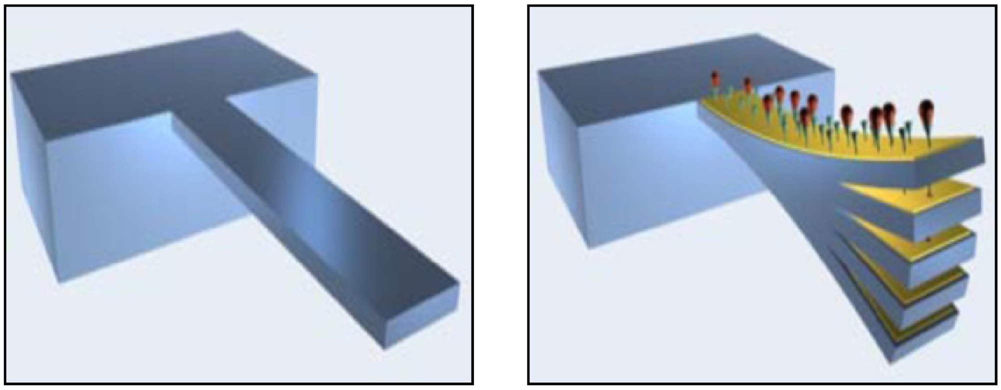

(a) (b)

Figure 2. MEMS Cantilever Sensor; (a) cantilever without binding mass, (b) cantilever deflects due to binding mass [Guillermo (2006)]

As the MEMS cantilever deflects, the resulted deformation is termed bending. External applied loads which cause bending will result in reactions at the free end, consisting of displacement or deflection, δ_{max} as shown in Fig.3. Maximum deflection during force applied for a beam that has constant cross section can be calculated using equation (1) [Cheng (1998), Benham et al. (1996)]. Fig.3 shows the schematic of cantilever deflection where it has one fixed end and one free end with force/mass applied.

$$\delta_{\max} = {}^{Fl^3}/_{3EI} \tag{1}$$

where δ_{max} is the maximum deflection, F is force applied, l is the cantilever length, E is the Young's Modulus for the cantilever material which in this research is silicon and I is the moment inertia for the cantilever.

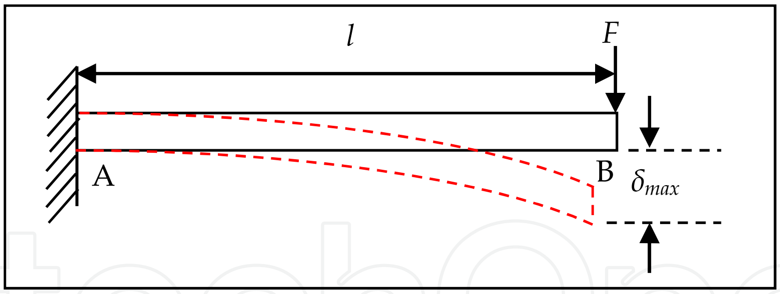

Figure 3. Schematic of MEMS cantilever deflection.

In the meanwhile, the cantilever will also sense stress that occurred during deflection. There are two type of stress occurred: tensile and compressive stress where tensile occurs at the top of cantilever and compression acts at the bottom of cantilever as illustrated in Fig.4. Since the piezoresistors are located at the top surface, research will be focuses at top surface of the cantilever.

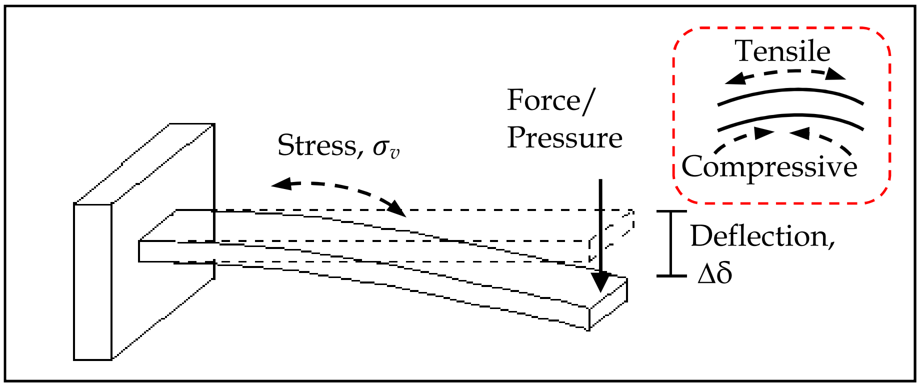

Figure 4. Stress occurred during force applied

Maximum stress can be calculated using equation (2) for a constant cross section beam.

$$\sigma_{max} = {}^{6Fl}/_{bh^2} \quad (2)$$

where *M, moment* = *F, force* x *l, cantilever length*, σ_{max} is the maximum stress, c is the height from the center axis to the top surface of the cantilever and *I*, moment of inertia.

3.1. Piezoresistive effect in silicon and MEMS cantilever relationship

Piezoresistive effect describes the changing electrical resistance of a material due to applied mechanical stress. The effect causes a change in resistance value. This effect has been used for semiconductor based sensor such as germanium, silicon and polycrystalline silicon. Silicon offers remarkable piezoresistive effect and it has controllability for electronic circuits [Madou (1997), Streetman and Banerjee (2006)]. Semiconductor silicon is the most common material in the MEMS field. Naturally, the electrical and mechanical properties of silicon are of great interest which differs from conductor (e.g. metals) and insulator (e.g. rubbers). It has a conductivity which lies between a perfect insulator and a perfect conductor. Liu (2006) states that the resistivity of semiconductor changes as a function of deformed mechanism. Therefore, silicon is a true piezoresistor. Liu (2006) also mentioned that piezoresistive effect refers to piezoresistor or resistor which changes during applied force or mass. The change in piezoresistance is linearly related to the applied stress and strain according to Bhatti et al. (2007) and Liu (2006). These related expressions are shown in equation (3) and (4) below [Chu et al. (2006)]:

$$\frac{\Delta R}{R} = \pi\sigma_l + \pi\sigma_t = \pi(\sigma_l - \sigma_t) \tag{3}$$

$$\frac{\Delta R}{R} = G.\frac{\Delta l}{l} \tag{4}$$

where ${}^{\Delta R}/_{R}$ is resistance change, σ_l and σ_t are the longitudinal and transverse stress components, π is the piezoresistive coefficient, G is gauge factor of piezoresistor (G=121, (Eklund and Shkel, 2007) , ${}^{\Delta l}/_{l}$ is strain component. From equation (3) above, it shows that resistance change increases by maximizing the differential stress $(\sigma_l - \sigma_t)$.

Resistance change, ${}^{\Delta R}/_{R}$ is often read using the Wheatstone bridge circuit configuration [Liu (2006)]. Wheatstone bridges consist of four resistors connected in a loop as shown in Fig. 5. An input voltage, V_{in} is applied across two junctions that are separated by two resistors. Voltage drop across the other two junctions forms the output [Hsu (2002), Boleystad (2003), Cook (1996)]. By locating the piezoresistive on the surface of a cantilever beam structure, a piezoresistive response can be correlated to the stress occurred as the MEMS cantilever deflect. Stress that occurs will be converted into voltage output, V_{out}.

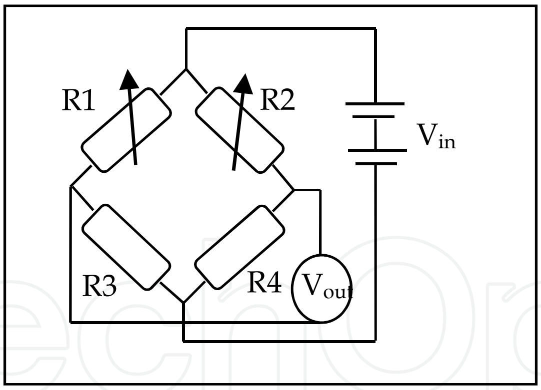

Figure 5. Wheatstone bridge circuit configuration; circuit consists of four piezoresistors in a loop [Cook (1996); Boylestad (2003); Chu et al.(2006)]

3.2. Piezoresistive MEMS cantilever design

In order to suit intended applications of MEMS cantilever, there are many available designs for MEMS cantilever. These designs vary in terms of the shape and parameter of the MEMS cantilever such as length, width, and thickness. In some published literatures, different designs at certain section of the MEMS cantilever are created where the shape is different from common MEMS cantilever design. Fig.6 shows the most common designs of piezoresistive MEMS cantilever available from literature studies such as rectangular shape, paddle pad and v-shape.

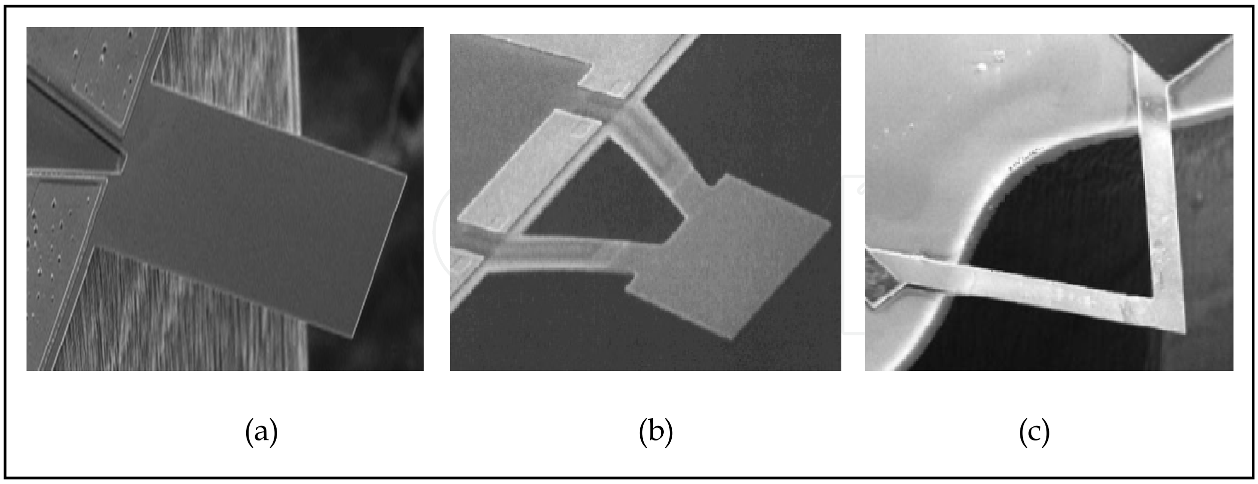

Figure 6. Type of shape for piezoresistive MEMS cantilever; (a) rectangle shape (b) paddle shape , (c) v-shape [Loui et al. (2008), Su et al. (1996), Saya et al. (2005)]

Additional designs or sections are proposed by some researchers to their fabricated device for the device protection according to the application purposes. Gel and Shimoyama (2004) have fabricated a protection head for their device to avoid the cantilever from easily being broken during handling as shown in Fig. 7(a). artificial hair cell (Fig. 7(b)) design are used for flow sensor as proposed by Fan et al. (2002).

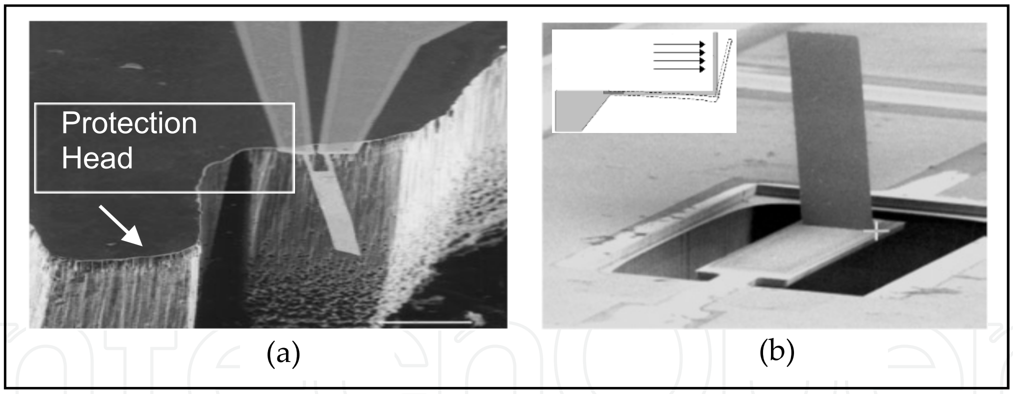

Figure 7. Additional design for MEMS cantilever; (a) protection head , (b) artificial hair cell [Gel and Shimoyama (2004), Fan et al. (2002)]

Table 1 summarizes MEMS cantilever designs shape, additional design, type of detection and also its applications. From the Table 1, it shows that a rectangular MEMS cantilever is a widely used for biosensor applications.

In this research, paddle pad type MEMS cantilever is chosen. The pad area is used as an area where force or mass can be applied or binding of biological mass. For rectangular type, the area for force or mass applied is smaller and it is difficult for the force to be applied. For safe handling during fabrication of the piezoresistive MEMS cantilever, the proposed design will also include the protection head.

References	Design/Shape	Additional design	Type of detection	Applications
Gel & Shimoyama (2004)	Rectangular	Protection head	Piezoresistive	Force sensing
Loui et al. (2008)	Square & trapezoidal	-	Piezoresistive	Chemical sensor
Park et al. (2007)	Paddle type	-	Piezoresistive	Acceleration sensor
Peiner et al. (2008)	Rectangular	Tip	Piezoresistive	Force sensor
Sone et al. (2004)	v-type	Triangle shape	Piezoresistive	Biosensor
Yoo et al. (2007)	Rectangular type	-	Piezoresistive and optical	Biosensor

Table 1. Summary of MEMS cantilever designs from literatures

3.3. Increasing the sensitivity of piezoresistive MEMS cantilever

There are several typical approaches to increase the sensitivity of piezoresistive MEMS cantilever as proposed in the published literature. The purpose of increasing the sensitivity for any MEM based device is to enhance the device capabilities to measure or detect small changes especially for biological mass detection which is to overcome low resolution of the read out system for piezoresistive detection method (Rosmazuin et al. (2008)).Table 2 summarizes the typical available approaches in order to increase sensitivity of piezoresistive MEMS cantilever. It looks like decreasing or making small dimension is the most popular approach in order to increase the sensitivity of piezoresistive MEMS cantilever. However, this approach requires high precision lithography and the equipment is very expensive, for example Micro/Nano Lithography machine. The same argument applied if the change to low Young's modulus material approach is taken. This approach needs deposition machine like LPCVD (low pressure chemical vapor deposition) or PECVD (plasma enhanced chemical vapor deposition) which is not available in many research labs. Another approach is by introducing stress concentration region (SCR).

References	Approach
Chivukula et al. (2006); Li et al. (2007); Jiang et al. (2008); Brugger et al. (1999); Pramanik et al. (2006)	Decrease geometry & use low doping level
Calleja et al. (2005)	Material changes (use low Young's modulus)
Yu et al. (2007); Bhatti et al. (2007); He and Li (2008)	Introduce stress concentration region (SCR)

Table 2. Summary of approaches taken to increase the sensitivity of MEMS cantilever

3.3.1. Stress concentration region (SCR)

The main concept for this approach is to increase stress that occurred in the cantilever. SCR is an approach where defects or holes are made in order to increase stress. To produce SCR, no extra high tech equipment is needed because it just involves etching and mask design. So, this approach appears to be the most suitable for enhancing the sensitivity of piezoresistive MEMS cantilever since the piezoresistive material has good sensitivity to stress and no additional complicated equipment or process are required.

Yu et al. (2007) introduced holes to the beam in their finite element analysis to study the effect of surface stress on the sensitivity of MEMS cantilever. The result shows that by introducing holes, the sensitivity of the piezoresistive MEMS cantilever can be increased. Fig.8 shows their result using ANSYS® where the maximum stress occurred near to the fixed end and at the last two SCR holes.

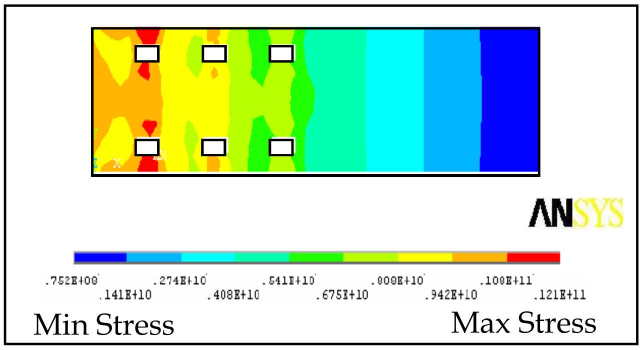

Figure 8. Surface stress effects along longitudinal distance cantilever with holes [Yu et al.(2007)]

Joshi et al. (2007) studied four types of SCR holes designs as shown in Fig.9 using Coventoreware2003. Long slit and staggered hole produced highest stress compared to other designs. It shows that more sharp corners can increase the stress occurred. This also agreed by He and Li (2006) which studied the surface stress effect on various types of SCR holes that are formed on the silicon cantilever using ANSYS®. Seven type of SCR holes shape have been analyzed such as rectangular, square, hexagonal, octagonal, circular and elliptical.

Table 3 summarizes the analysis result of surface stress or average stress difference for different types of SCR holes. The result shows that as the number of sides for SCR holes increases, the surface stress increases. The octagonal type of SCR holes gives the highest stress as it has the highest number of sides that creates surface stress.

He and Li (2006) also investigated the effect of adding more octagonal holes to the cantilever. Table 4 shows the surface stress occurred at SCR holes when different numbers of SCR holes of the same size are added along the length of the cantilever with the same spacing between the SCR holes. It shows that adding more SCR holes to the cantilever does not help to enhance the surface stress. Hence one octagonal SCR hole is enough to maximize the surface stress.

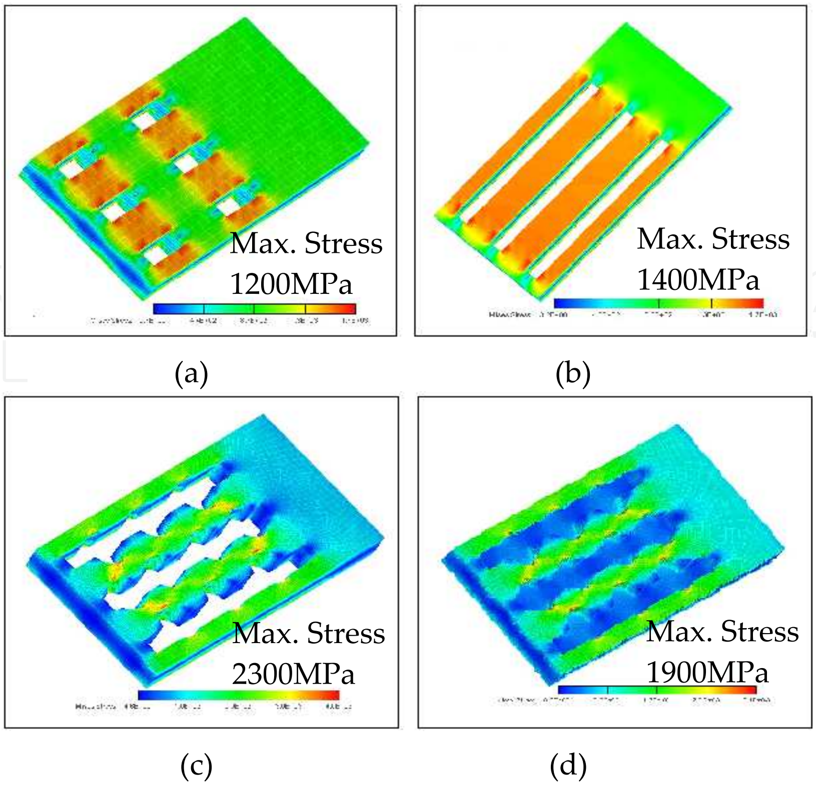

Figure 9. Coventorware 2003 analysis, (a) six rectangular hole type, (b) long rectangular slit, (c) long slit and staggered holes, (d) Partially-etched SCR [Joshi et al. (2007)]

Shape of SCR holes	Maximum Stress (MPa)
Cantilever without any hole	439
Rectangular	589
Square	563
Hexagonal	591
Octagonal	690
Circular	621
Elliptical	590

Table 3. Maximum stress for different shape of SCR holes [He and Li (2006)]

No. of Holes	Maximum Stress (MPa)
0	439.00
1	689.76
2	686.48
3	686.86
4	686.91

Table 4. Maximum stress when adding number of octagonal SCR holes [He and Li (2006)]

Bhatti et al. (2007) also simulated piezoresistive MEMS cantilever with paddle pad with rectangular SCR holes by adding the number of SCR holes. Table 5 shows the summary of the result on the effect of adding the number of rectangular SCR holes to the piezoresistive MEMS cantilever with paddle pad as shown in Fig.10. From the table, it shows that surface stress increases when one rectangular SCR holes is introduced. When adding more SCR holes to the cantilever, the surface stress does not change much. Compared with He and Li (2006), Bhatti et al. (2007) have the same surface stress behaviour when adding more SCR holes as shown in Fig.10. Both studies agreed that adding more SCR holes does not affect the surface stress; this happen because when a cantilever deflects, the bending moment is maximum at the fixed end. Hence the stress only shows significant increment at the first hole which is near to the fixed end because the sensitivity of piezoresistive MEMS cantilever cannot be further increased. In order to increase the sensitivity, one SCR hole is sufficient.

No. of Holes	Maximum Stress (MPa)
0	72.47
1	159.66
2	154.93
3	154.19
4	153.89

Table 5. Maximum stress with increasing the no. of SCR holes [Bhatti et al. (2007)]

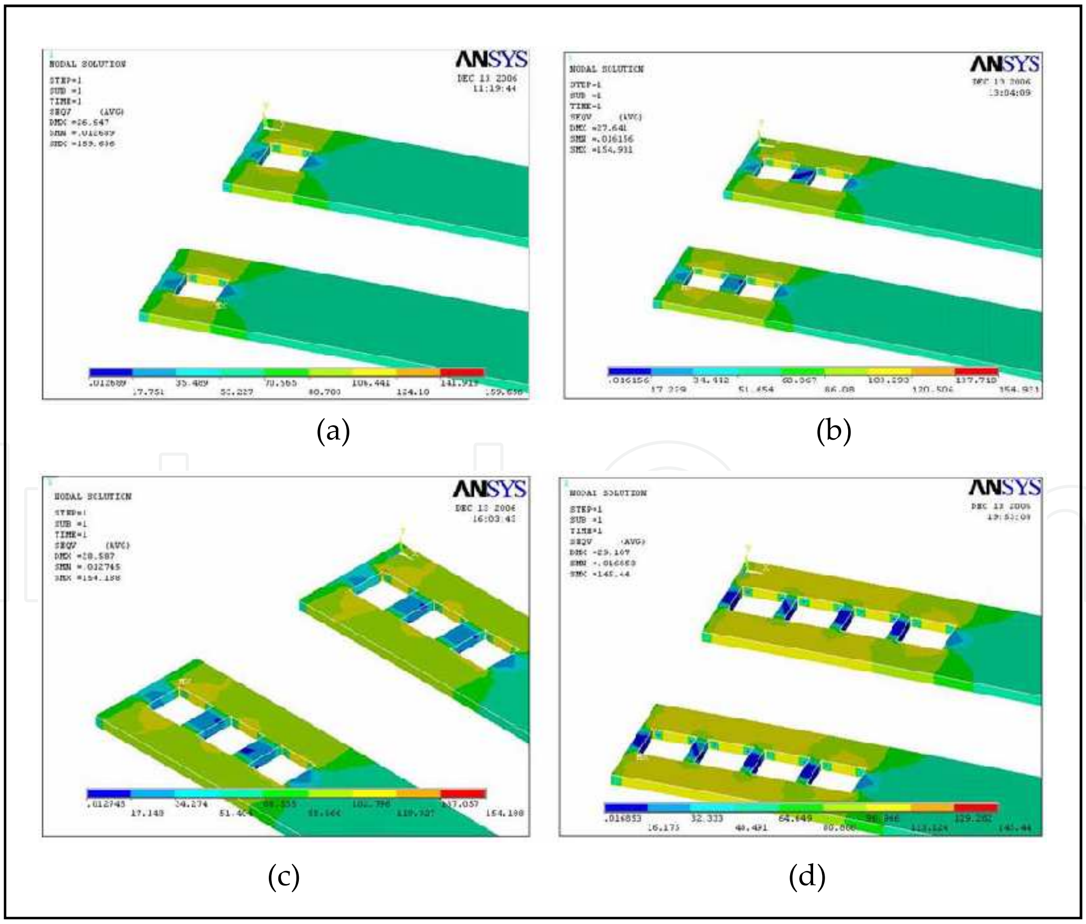

Figure 10. Cantilever stress distribution when adding SCR holes, (a) 1 hole, (b) 2 holes, (c) 3 holes, (d) 4 holes [Bhatti et al. (2007)]

In this research, all rectangular, hexagon, octagonal and decagonal types of SCR holes proposed by He and Li (2006) are selected for fabrication in order to increase the sensitivity and also to select which design is suitable with FEA and fabrication process. However the main problem of past literatures that used SCR method was most of the designs only did FEA simulation only and the study did not compared with the fabricated designs.

3.4. Location of piezoresistors to form Wheatstone bridge circuit

Conventionally, the piezoresistors are placed on the MEMS cantilever as close as possible to its clamped edge or fixed end. Fuller (2007) mentioned that the location of piezoresistor is best suited wherever the maximum stress occurs. Thus, the maximum stress that piezoresistors will sense is the maximum stress on the MEMS cantilever structure. Wheatstone bridge circuit configuration, there are two type of piezoresistors; the active type will be located at the high stress area whereas the passive type will be located at near zero stress area as illustrated in Fig.11 [Behren et al. (2003), Chu et al. (2007)]. The location of piezoresistor can be determined using FEA which will be discussed further in next section.

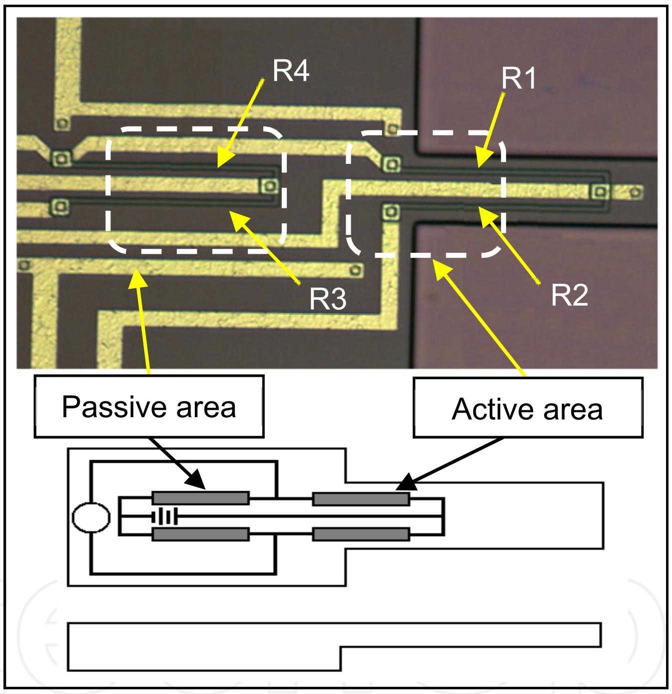

Figure 11. Passive and active area for piezoresistors location [Chu et al. (2007)]

3.5. Modelling and design of piezoresistive MEMS cantilever

Paddle type rectangular cantilever is chosen for this research since it has large area for mass binding or to apply external load onto its paddle pad. The selection of SCR designs base on past literature, then simulate to determine the stress characteristics. From the FEA results, the SCR designs are fabricated and not all designs suit with the fabrication process. The polygon SCR tend to be circular shape due to low SCR dimension and etching process interaction that over-etch the side SCR shape.

Two paddle type piezoresistive MEMS cantilevers were modeled using computer aided design (CAD) software Solidwork®. Those types are:

- Solid piezoresistive MEMS cantilever paddle pad model as shown in Fig.12a
- Piezoresistive MEMS cantilever paddle pad with stress concentration region (SCR) model as shown in Fig.12b

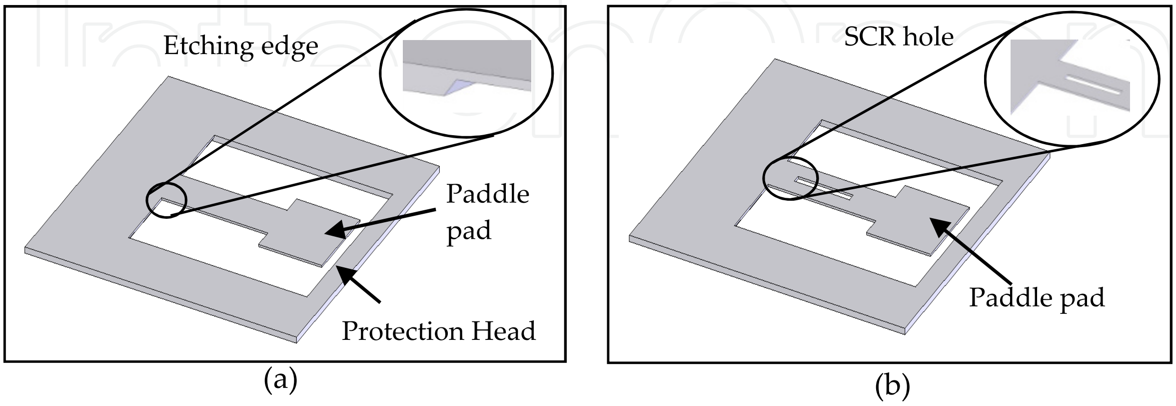

Figure 12. Piezoresistive MEMS cantilever model using Solidwork®;

Fig.13 shows the detailed drawing of piezoresistive MEMS cantilever model that is analyzed using ANSYS®. The dimensions were taken from the successful model of piezoresistive MEMS cantilever that was fabricated in the cleanroom for this research. The red line represents path line location that has been used for detail stress distribution and deflection profile plot.

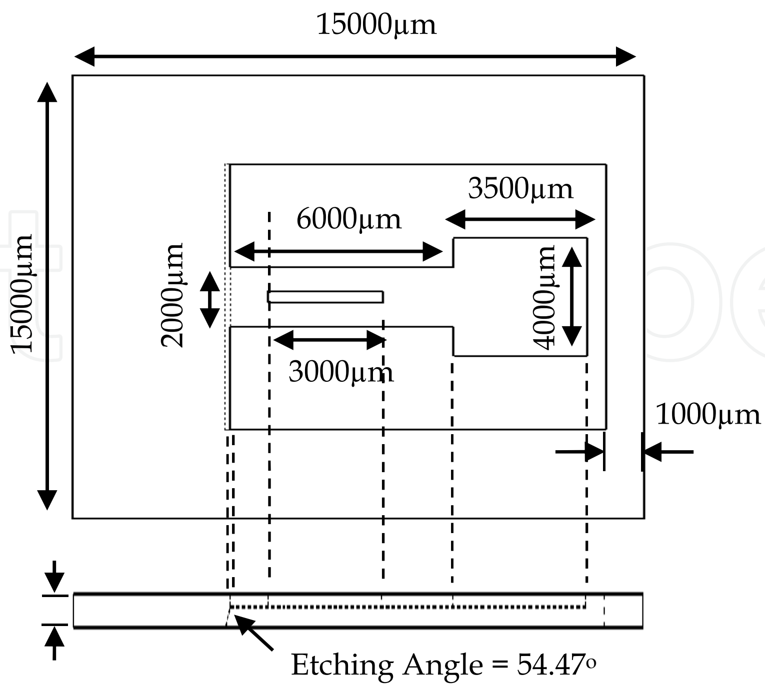

Figure 13. Detailed drawing for piezoresistive MEMS cantilever with paddle pad model

3.6. Finite element analysis (FEA) using ANSYS®

The piezoresistive MEMS cantilever model analysis is carried out by using ANSYS® version 9.0. The analysis is carried out to investigate and understand the stress and deflection of the piezoresistive MEMS cantilever when external pressure or load is applied. First, the model files were imported from Solidworks® into ANSYS® software so that there will be no error during analysis. The model of interest must be prepared in a manner where the solver will understand.

Then pre-processing is the second step and it is an important step when using ANSYS® prior to any solution execution. Some pre-processing procedures involved during analysis of piezoresistive MEMS cantilever models will be discussed here, including:

- **Element type**

  The proper selection of element is important to ensure desired analysis is carried out. The chosen element must be an elastic element with constant performance and suitable with the computer performance. Several types of element have been tested in order to suit the piezoresistive MEMS cantilever models, with the result verification and also along with computer performance so that the analysis would be finely carried out. Behrens et al. (2003) mentioned that tetrahedral element SOLID187 fits best to the shape of structure fabricated by anisotropic etching. After some verification with the available cantilever models in the literature [Bahtti et al. (2007), Yu et al. (2007)], the SOLID187 element was chosen as the element type.

- **Material properties**

  For this analysis, material properties used throughout both models are called linear properties. Linear properties are chosen because the analysis with these properties requires only a single iteration and not temperature dependent. The material is also defined as isotropic which means the same mechanical properties are applied in all directions. Silicon material will be used during fabrication of piezoresistive MEMS cantilever. Therefore, silicon properties are applied for ANSYS® models. Table 6 lists the material properties of silicon used for piezoresistive MEMS cantilever models.

Properties	Value	Reference
Young's Modulus	150GPa	Yu et al. (2007)
Poison's ratio	0.22	Yu et al. (2007)
Density	2280 kg/m^3	Yu et al. (2007)

Table 6. Material properties used in ANSYS®

- **Meshing**

  The piezoresistive MEMS cantilever models are meshed by free meshing. Arik et al. (1999) have study the meshing effect for fine and coarse mesh structure. The results show that there is no major difference in both solutions. In this research, the analysis used coarse mesh in order to save time and to avoid crash during analysis. Table 7 lists the number of elements and node counted for both piezoresistive MEMS cantilever design. An element is a form of several nodes. For piezoresistive MEMS cantilever with SCR holes, number of nodes and elements are higher than solid cantilever because at the SCR holes the element are more refine. Fig.14 illustrates free meshed for both piezoresistive MEMS cantilever models.

Design	No. of Nodes	No. of Elements
Solid Cantilever	9365	4212
Cantilever with SCR hole	9813	4389

Table 7. Number of elements and nodes

- **Boundary conditions**

  Before solutions can be initiated, constraints or boundary conditions need to be imposed. Boundary conditions are a selected area or body that will be fixed with no displacement in any degree of freedom or any direction (DOF). When load is applied, the selected boundary condition area will remain constant which mean no deflection or movement occurred. In ANSYS®, boundary conditions or constraints are usually referred to as loads where the scope includes setting of boundary conditions (constraints, supports or boundary field specification) as well as other externally and internally applied loads. Most of these loads can be applied on the solid model (keypoints, lines, areas, and volume) or the finite element models (nodes and elements).

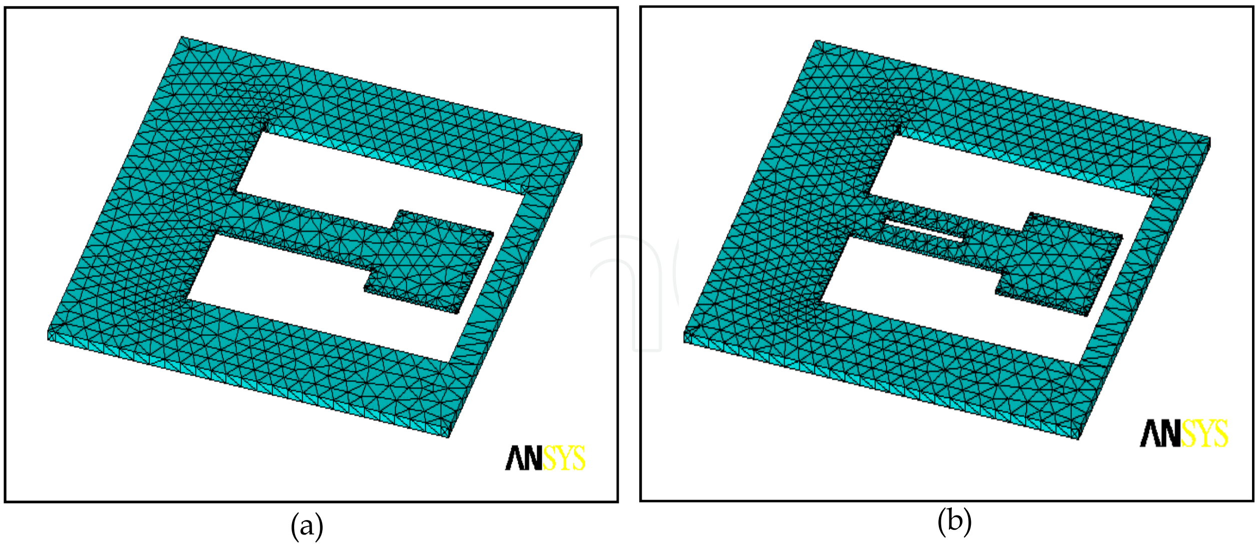

Figure 14. Element plot after meshing for piezoresistive MEMS cantilever: (a) solid cantilever, (b) cantilever with SCR hole

For this research, both models are constrained (zero DOF) in x, y, and z direction on the area as shown in Fig.15. Only the MEMS cantilever structure will reflect to the applied load.

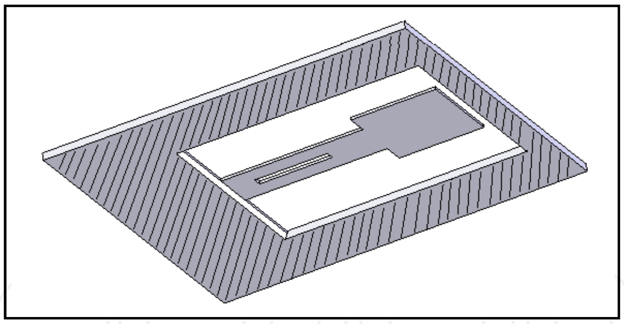

Figure 15. Selected area for boundary condition or constraint

- **Pressure applied and Contact area**

  In order to make the piezoresistive MEMS cantilever deflect, external force or mass should be applied at the free end area. From the literature, the external force or mass value depends on the limitation of the cantilever itself which means the smaller the cantilever geometry the lower is the force or mass it can detect or be applied. For this research, force or mass applied represents biological mass that is commonly applied for biosensor/ cantilever application [Yu et al. (2007), Vashist (2007)]. The mass value is converted to pressure so that it can suit with ANSYS®. The pressure will be applied on the paddle pad area only which is at the free end. Mass from 0 up to 5gram has been chosen for this analysis.

The conversion of pressure value is carried out using equation (5).

$$P = {}^{mg}/_{A} \tag{5}$$

where P is pressure, mg is force and A is the applied area.

Table 8 lists the converted mass applied to pressure for ANSYS® analysis.

Mass (g)	Area (m^2) x10^{-5}	Pressure (Pa)
0	1.5	0
0.2	1.5	130.67
0.4	1.5	261.33
0.6	1.5	392.67
0.8	1.5	523.33
1.0	1.5	654.00
1.5	1.5	981.33
2.0	1.5	1308.00
2.5	1.5	1635.33
3.0	1.5	1962.00
3.5	1.5	2289.33
4.0	1.5	2616.00
4.5	1.5	2943.00
5.0	1.5	3270.00

Table 8. Converted mass applied to pressure for ANSYS® analysis

The pressure is applied on the area at the cantilever free end. Fig.16 illustrates the area where the pressure is applied on the piezoresistive MEMS cantilever models for ANSYS® analysis.

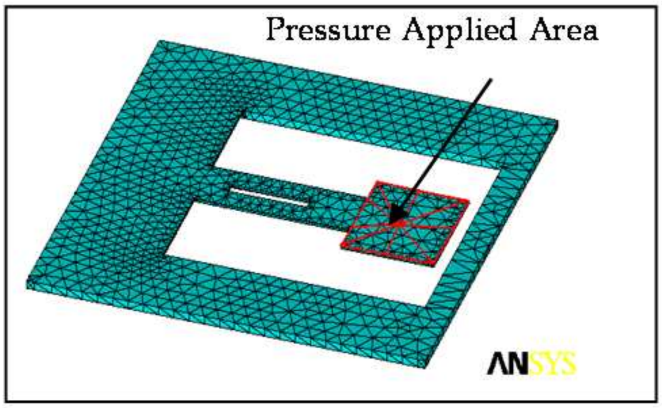

Figure 16. Pressure applied area for ANSYS® analysis

3.7. Wheatstone bridge circuit (piezoresistive circuit) analysis

The Wheatstone bridge has been used extensively in the literature to determine the output voltage for piezoresistive MEMS cantilever. Cook (1996) mentioned that Wheatstone bridge is commonly used for gathering and measuring the electrical signal generated from gauges. It consists of four resistors connected together and one of the resistors will be acting like the strain gauge. Fig.17 shows the Wheatstone bridge configuration in schematic diagram.

R1 is the active resistor and measuring gauge and the other three resistors are the passive resistors. Any variation in the current in the middle resistor will cause a change in output voltage from the circuit. In this research, software for circuit analysis named MultiSIM8® is used in order to study the circuit characteristic. Fig.17 shows the Wheatstone bridge circuit configuration using MultiSIM®. At ease, the circuit multimeter will show zero voltage as shown in Fig.17(a) and when the piezoresistive MEMS cantilever senses any stress at R1, the output voltage will change as shown in Fig.17(b). The resistance values are not fixed at any values. Hence any value can be taken as long as the measured output voltage is zero.

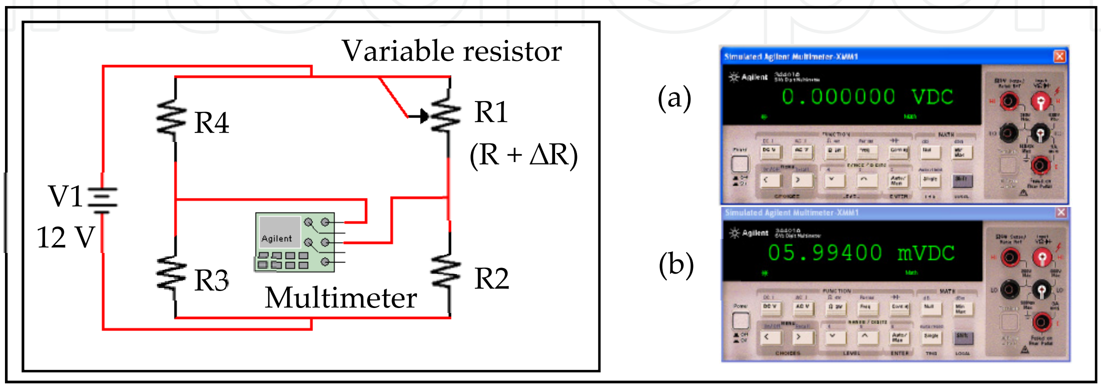

Figure 17. Wheatstone bridge configuration using MultiSIM®

3.8. Summary of fabrication and testing

In this research, two types of piezoresistive MEMS cantilever will be fabricated; solid design and 3mm SCR design piezoresistive MEMS cantilever. Fig.18 exemplifies the processes sequence schematically for piezoresistive MEMS cantilever fabrication.

Successful fabricated piezoresistive MEMS cantilever is shown in Fig.19. In this figure, two types of piezoresistive MEMS cantilever; without SCR and with rectangular SCR design had been fabricated which basically has 9500μm length, 2000μm width (4000μm X 3500μm for paddle pad) and 100μm thick. Other than these two cantilevers, protecting heads have also been successfully fabricated for handling safety during fabrication processes and testing.

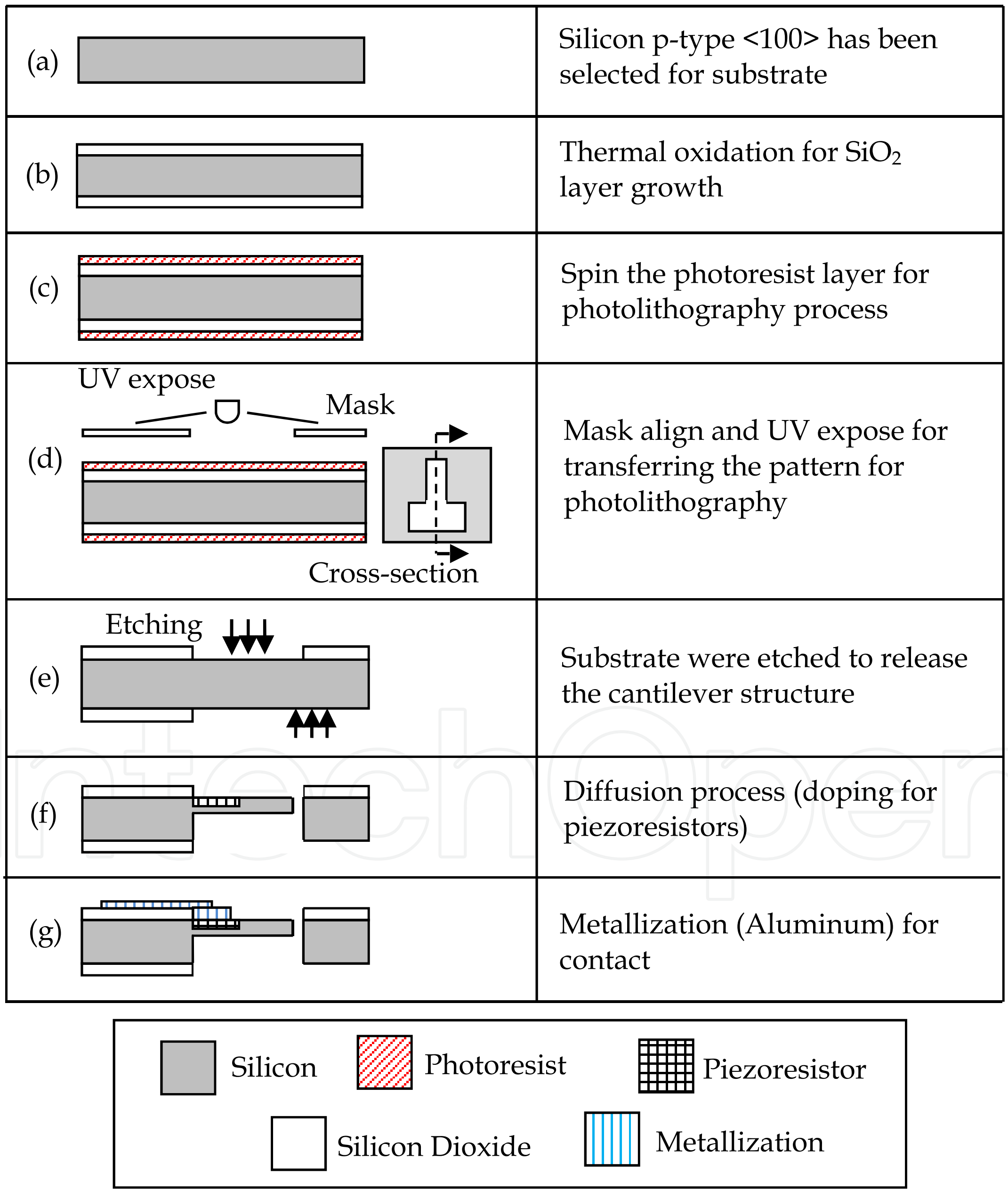

Figure 18. Fabrication of piezoresistive MEMS cantilever

Further Current-Voltage test (I-V test) was used to characterize the fabricated piezoresistors for piezoresistive MEMS cantilever as illustrated in Fig.20. Each piezoresistor was tested by applying voltage from -10volt to 10volt across piezoresistor and the resulting current was measured.

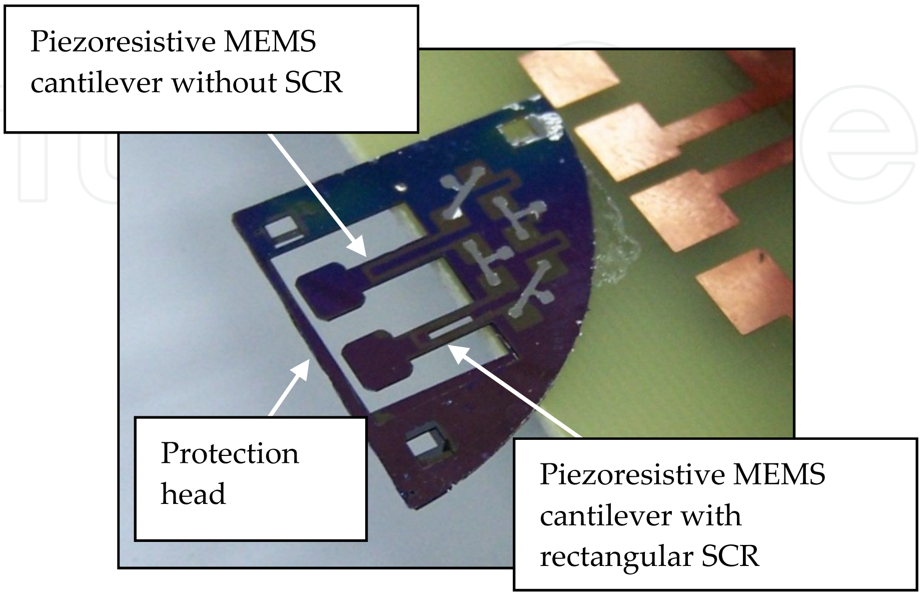

Figure 19. Successful fabricated solid and SCR piezoresistive MEMS cantilevers.

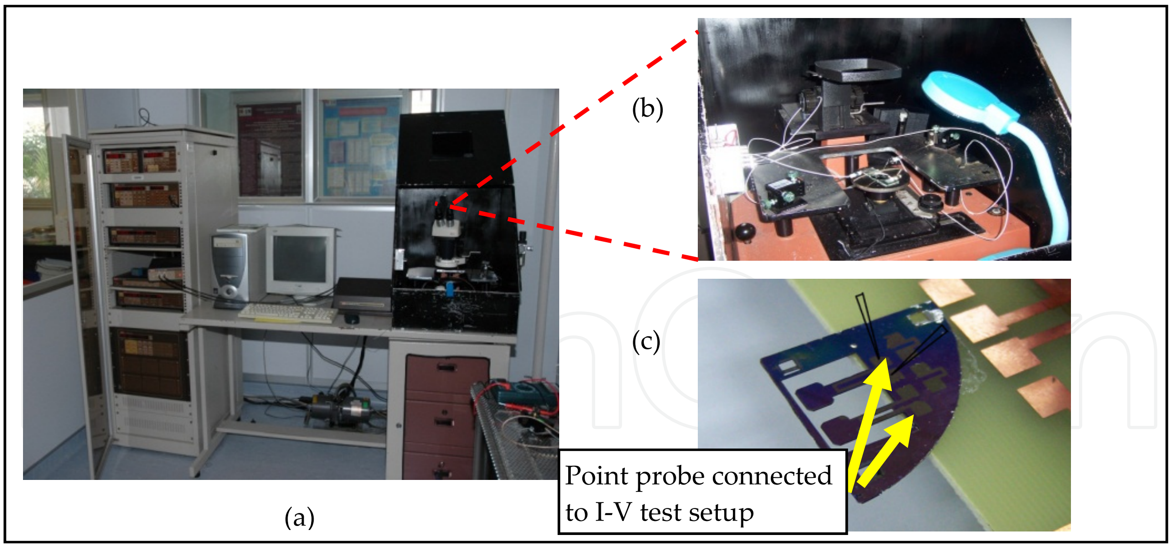

Figure 20. I-V test setup: (a) test setup system, (b) Point probe setup and magnifying glass, (c) Point probe connected to piezoresistor

4. Results and discussions

Results from the methodologies given in the earlier section are presented and discussed accordingly.

- Analysis on piezoresistive MEMS cantilever without SCR
- Selection of SCR designs for piezoresistive MEMS cantilever
- Analysis on cantilever without SCR and cantilever with selected SCR design
- Analysis on fraction change of piezoresistor using MultiSIM®
- Analysis of fabricated piezoresistive MEMS cantilever

4.1. Analysis on piezoresistive MEMS cantilever without SCR

As mentioned in the previous section, the mass applied from 0 to 5gram is converted to pressure during FE analysis throughout this research. From the results of the analysis, it can be deduced that the stress increases with the increase of the mass applied in a linear fashion of the maximum stress when mass is applied compared with calculation were not more 10% different as shown in Fig.21(a). Stress contour obtained when 1g mass is applied on the paddle pad area of the piezoresistive MEMS cantilever without SCR is shown in Fig.21(b). Maximum stress occurs at the cantilever fixed end. It shows that the cantilever has high bending moment at the fixed end.

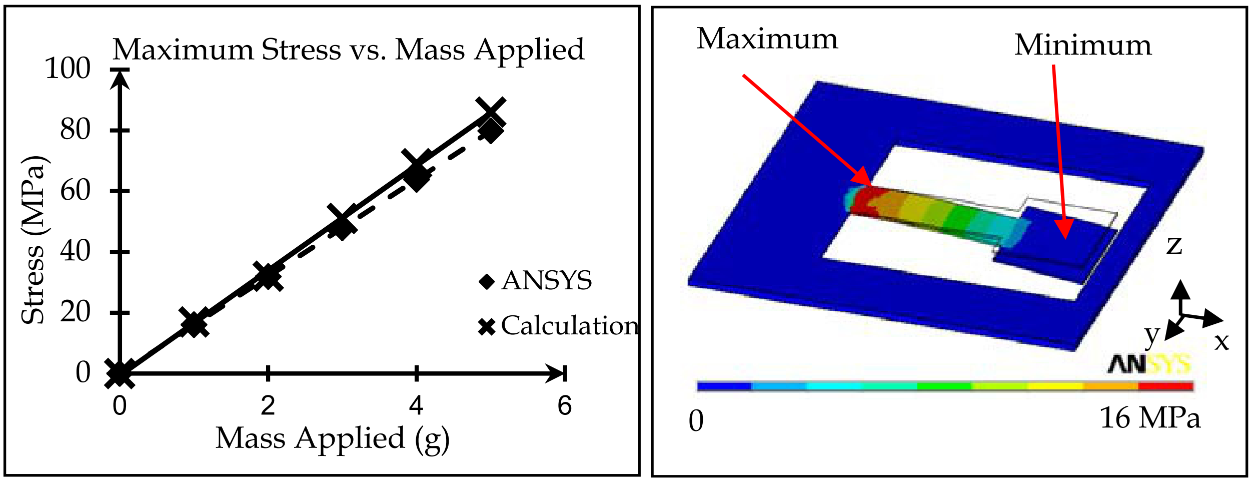

(a) (b)

Figure 21. Maximum stress for piezoresistive MEMS cantilever without SCR when varying mass is applied; (a) max. stress plot, (b) stress contour when 1gram mass applied

Liu (2006) mentioned that the maximum stress associated with the individual cross sections changes linearly with respect to the distance to the free end. Stress occurs at the top and bottom surface then decrease when approaching to the middle of cantilever thickness. Fig.22 illustrates stress distribution along the cantilever length when force/mass is applied at the free end. Fig.22 also illustrates stress distribution along the cantilever thickness when force/mass is applied at the free end. This verifies that maximum stress is high at the fixed end and it is this reason piezoresistors are commonly fabricated on the surface of the cantilever and near to the fixed end.

Results from equation (1) and ANSYS® simulation were plotted in Fig.23. Both results show linear trend results where the increase of mass applied would increase the maximum deflection of solid piezoresistive MEMS cantilever.

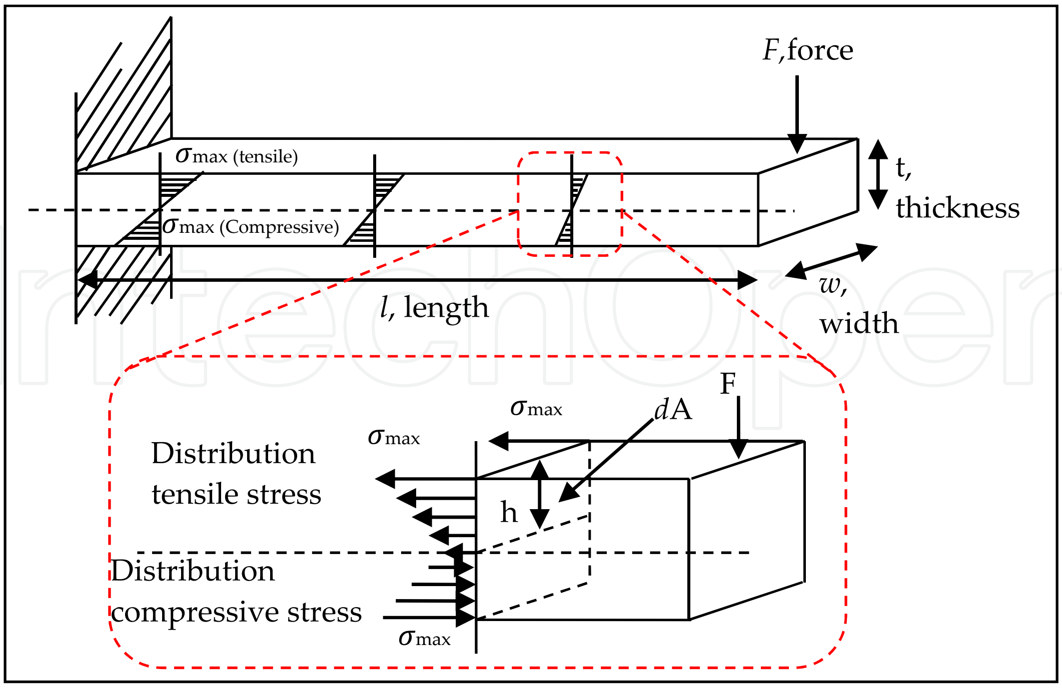

Figure 22. Stress distributions along the cantilever thickness when force or mass applied [Liu (2006)].

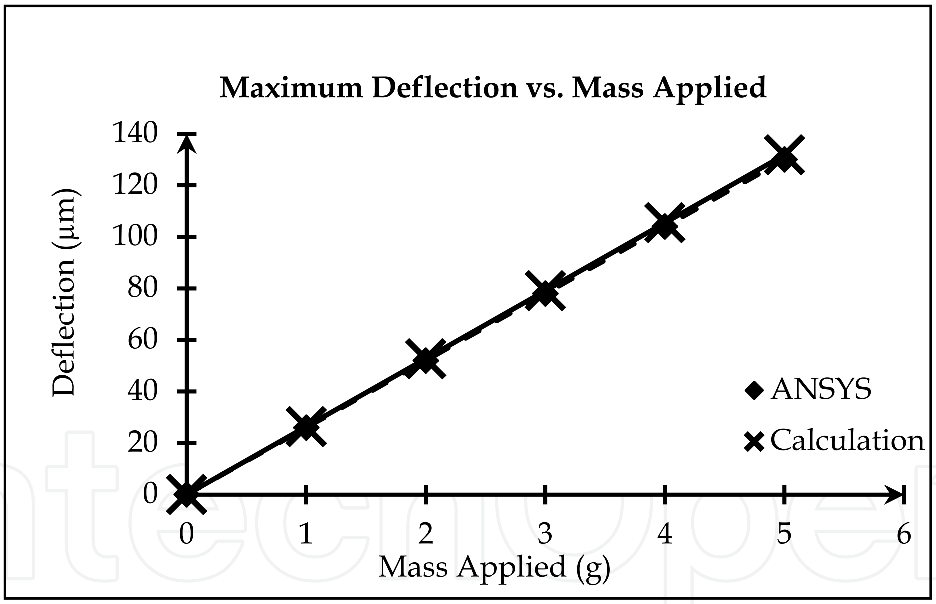

Figure 23. Maximum deflection plot with varying mass is applied.

4.1.1. Stress distribution and deflection profile along a path line for piezoresistive MEMS cantilever without SCR

When plotting stress along the selected path, a detailed stress and deflection analysis can be studied. Fig.24 shows the stress distribution along the path when a 1g mass is applied at the free end of the piezoresistive MEMS cantilever without SCR. It also shows the stress occurs throughout the path line where the maximum stress of 16.2MPa occurs at the fixed end as shown in Fig.24(a). From the path plot the maximum stress occurs at the fixed end which is in good agreement with Liu (2006) in previous section.

Fig.24(b) illustrates deflection plot along the path line for 1g mass applied. Combining the path stress and deflection plot, the piezoresistive MEMS cantilever starts to deflect at the location of maximum stress. From the path plot, the maximum deflection of 70.2μm occurs at the free end of the cantilever as shown in Fig.24(b). The same plot pattern has been obtained by Behrens et al. (2003) for their piezoresistive MEMS cantilever model along the longitudinal distance when a 20μN load is applied at the free end. In this research, MEMS cantilever deflection was not the main consideration because the piezoresistive method is highly depend on stress occurred. Hence the research is focused more to stress characterization.

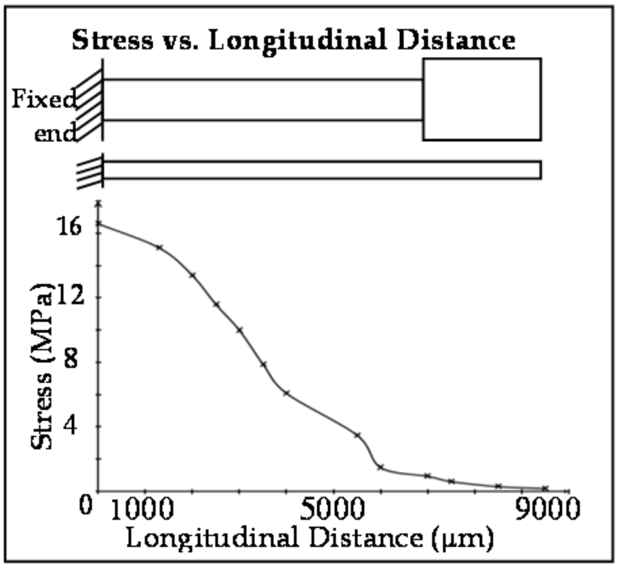

(a)

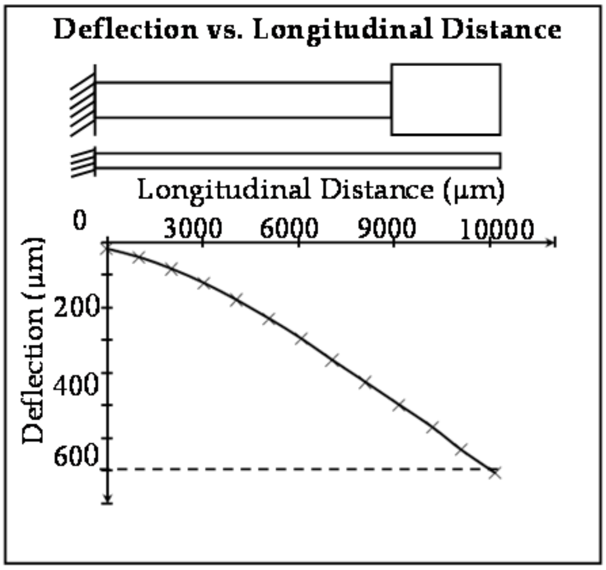

(b)

Figure 24. Stress through along the path line plot for piezoresistive MEMS cantilever without SCR when 1g mass applied.

4.2. Analysis on rectangular, hexagonal and octagonal SCR designs of piezoresistive MEMS cantilever

Three types of SCR designs have been choose from the past literature to study their stress characteristic when the mass is applied. Fig.25 shows the cantilever models with SCR designs dimensions.

Fig.26 shows the comparison between MEMS cantilever without SCR and MEMS cantilevers with SCR designs when varying mass is applied. From the plot, all SCR designs successfully increase the stress occurred at the cantilever. As the number of sides increase, the stress occurred also increases except rectangular SCR since its length of 1000μm will remain constant. Rectangular SCR designs have the highest stress plot but between these two designs, rectangular SCR design is selected due to its suitability with photolithography and etching process.

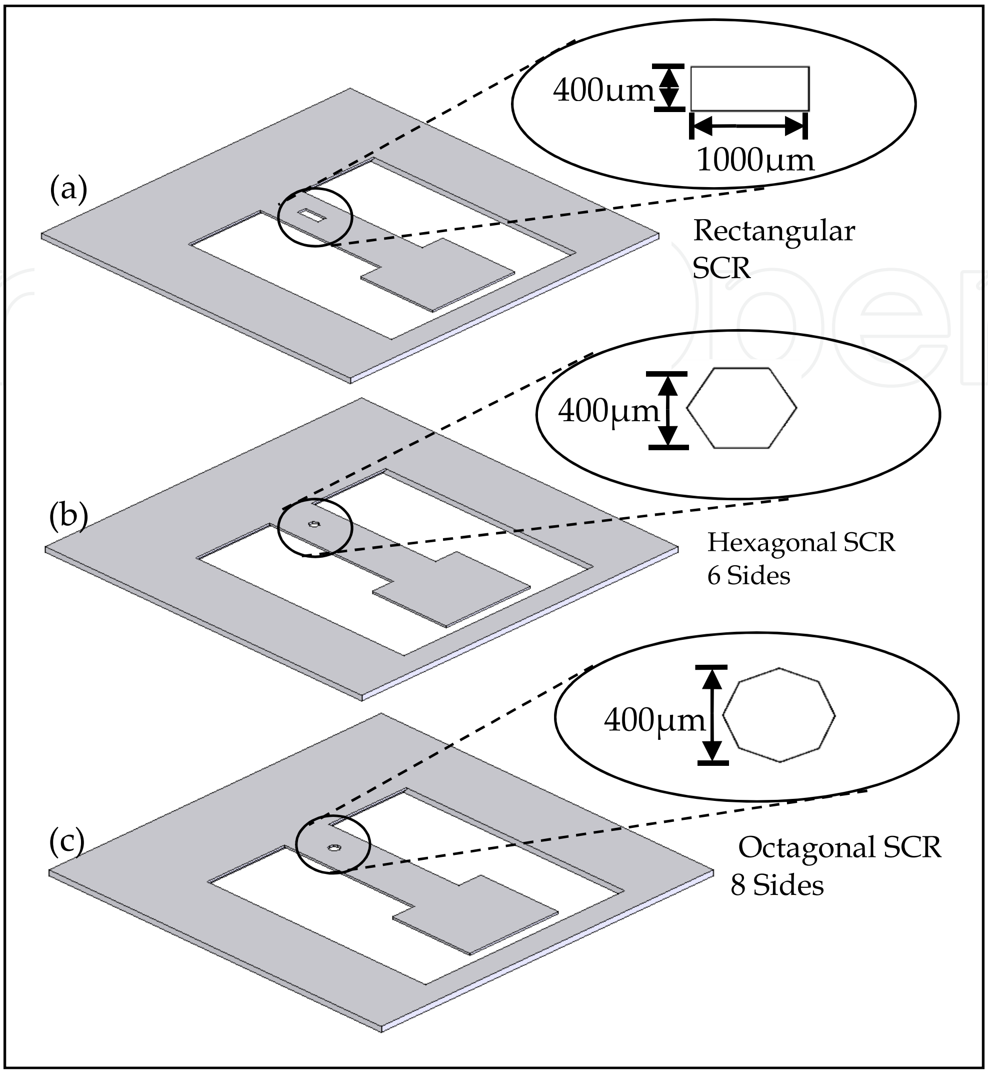

Figure 25. Piezoresistive MEMS cantilever with SCR designs: (a) rectangular, (b) hexagon, (c) octagonal

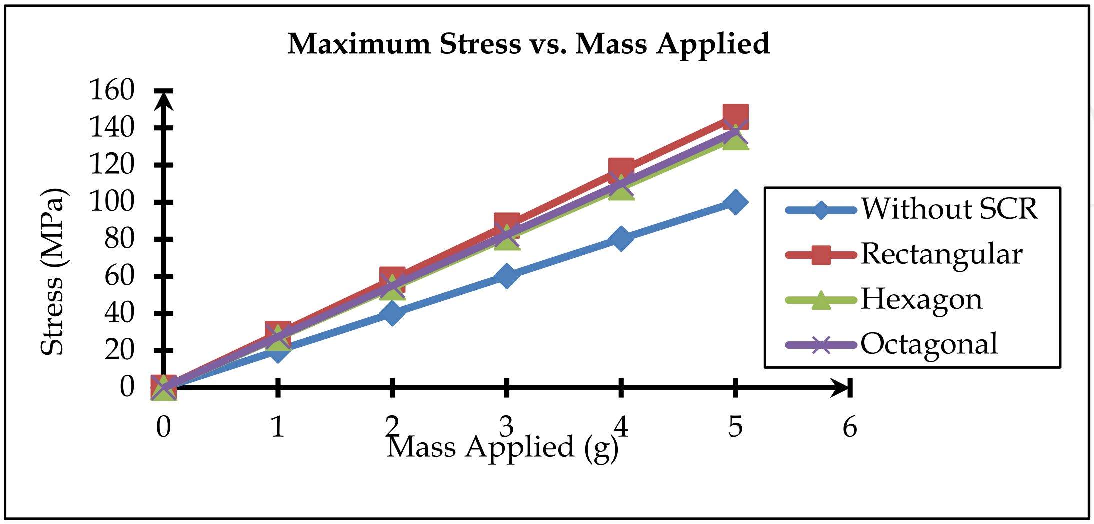

Figure 26. Maximum stress for piezoresistive MEMS cantilever without SCR and with various SCR designs for varying mass applied

4.3. Analysis on piezoresistive MEMS cantilever with various rectangular SCR dimensions

As mentioned earlier in the previous section, rectangular SCR design has been selected for detailed stress study where the length of rectangular SCR hole with constant width (400μm) is increased from 1000μm to 3000μm. All piezoresistive MEMS cantilever with rectangular SCR designs are compared with the MEMS cantilever without SCR in order to determine which rectangular SCR design will develop the highest stress. The selected design will be fabricated along with piezoresistive MEMS cantilever without SCR for characterization and functionality testing.

Fig.27 show the stress distribution plot along the path line is plotted for piezoresistive MEMS cantilever without SCR and all piezoresistive MEMS cantilever with rectangular designs when 1g mass applied. All piezoresistive MEMS cantilever with rectangular SCR has higher stress at the fixed end compared to piezoresistive MEMS cantilever without SCR. The stress occurred also increase along the length of rectangular SCR as the length increase. This shows that by increasing the length of rectangular SCR, the stress along the cantilever is also increased. It shows that piezoresistive MEMS cantilever with rectangular SCR A3 is the most suitable to fabricate since the increase in stress is more compared to rectangular SCR A1design and rectangular SCR A2 design.

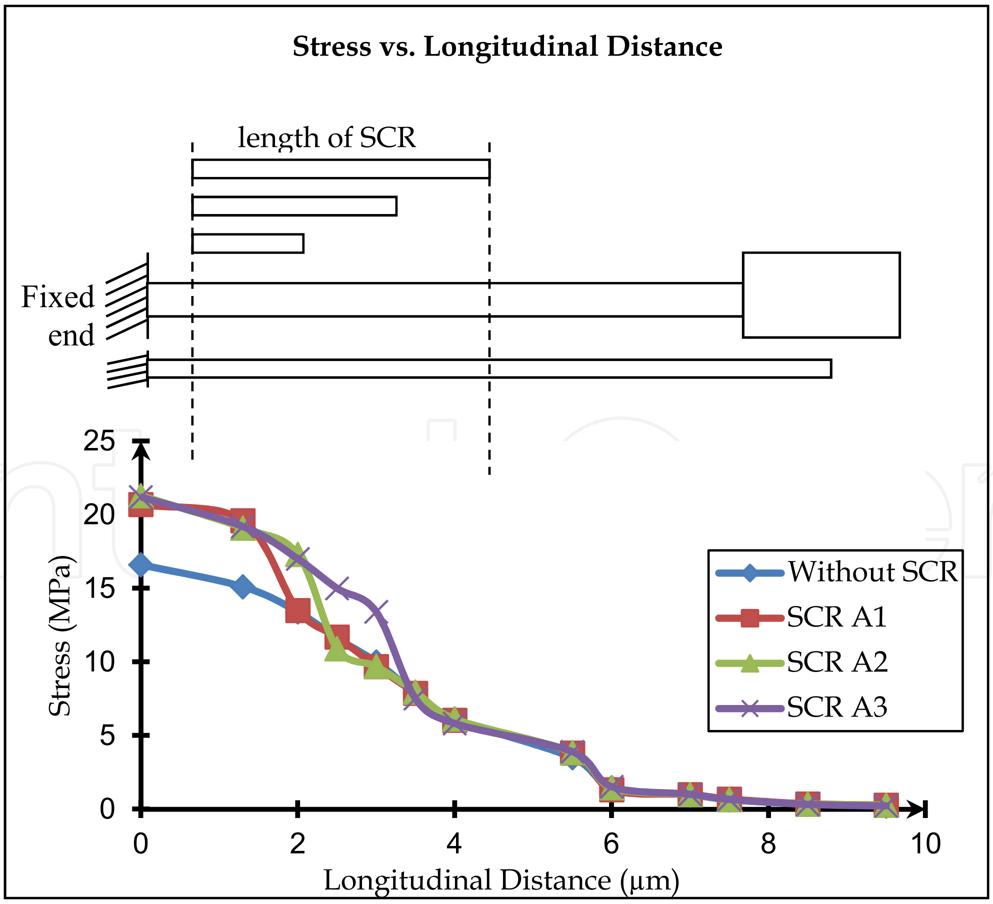

Figure 27. Stress along the path line plot for piezoresistive MEMS cantilever without SCR and piezoresistive MEMS cantilever with rectangular SCR designs when 1g mass applied.

Hence, the piezoresistive MEMS cantilever with rectangular SCR A3 design and piezoresistive MEMS cantilever without SCR will be used for Wheatstone bridge circuit analysis using MultiSIM®. Both piezoresistive MEMS cantilever designs will also be fabricated and tested

4.4 .Analysis on output voltage of piezoresistors using MultiSIMS®

Data from FEA were used for the piezoresistor circuit testing using MultiSIM® software. Fig.28 shows the graph of output voltage when mass is applied at the free end. The output voltage increases with the increase of mass applied. The piezoresistive MEMS cantilever without SCR seems to be less sensitive than the piezoresistive MEMS cantilever with rectangular SCR A3. This shows that by introducing rectangular SCR A3 to the piezoresistive MEMS cantilever can increase the sensitivity compared to the piezoresistive MEMS cantilever without SCR. Chu et al. (2007) also obtained a linear relationship for the output voltage versus applied force. Results shows that by introducing rectangular SCR A3 to the piezoresistive MEMS cantilever, the sensitivity is enhanced by almost about 2 times.

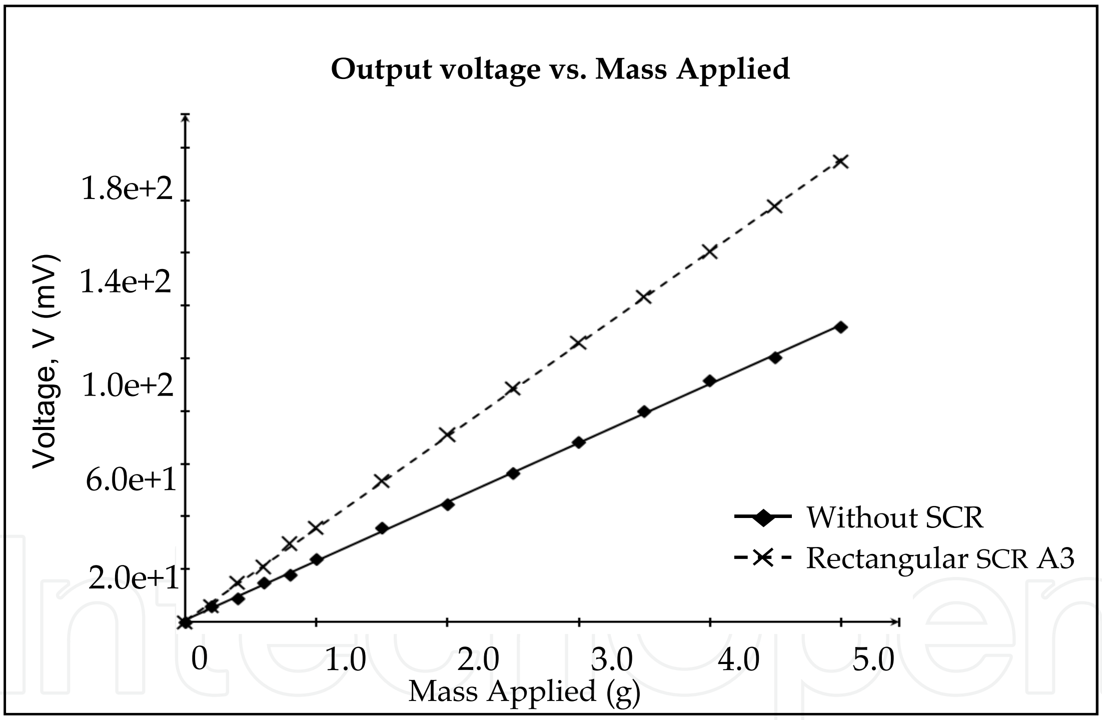

Figure 28. Output voltages when varying mass applied

4.5. Fabricated piezoresistive MEMS cantilever testing

Both fabricated piezoresistive MEMS cantilevers have been tested with 1, 2 and 3 gram of mass. Mass was applied at the paddle pad free end of the piezoresistive MEMS cantilever without SCR and with rectangular SCR A3 design. The output voltage change with varying mass applied was measured by Wheatstone bridge (WB) test setup as shown in the previous section. Fig.29 shows the output voltage from the Wheatstone bridge circuit when varying mass is applied for the fabricated piezoresistive MEMS cantilever without SCR and with rectangular SCR A3 design. Results show that both cantilever have polynomial relation, hence trend line is added for both curve fitting. From the R^2 values, both were near to 1 which mean the trend line almost balance through all plotted data. The output voltage not linear due to environment effect since the fabricated Wheatstone bridge circuit is sensitive to any changes in temperature. Chu et al. (2007) obtained linear relationship for output voltage versus applied force. From plotted results, the average sensitivity for piezoresistive MEMS cantilever with rectangular SCR A3 was $0.063 mVg^{-1}$ and $0.032 mVg^{-1}$ for the piezoresistive MEMS cantilever without SCR. When comparing both values, the piezoresistive MEMS cantilever with rectangular SCR A3 has successfully enhanced the sensitivity by 1.97 times from the piezoresistive MEMS cantilever without SCR.

Comparing the sensitivity value determined from MultiSIM® analysis, 2 times and fabricated device, 1.97 times, both results show that by introducing rectangular SCR A3 to the piezoresistive MEMS cantilever the sensitivity has successfully enhanced. The difference between both sensitivity is 1.5%. The different results obtained for both fabricated piezoresistive MEMS cantilever are due to uncontrollable fabrication processes such as etching rate, doping concentration, photolithography effect and the difference in the value of Young's Modulus etc. Besides that, environmental conditions like cleanroom temperature and vibration disturbance are also among enforcing effect because low dimension sensor has high sensitivity with the surrounding.

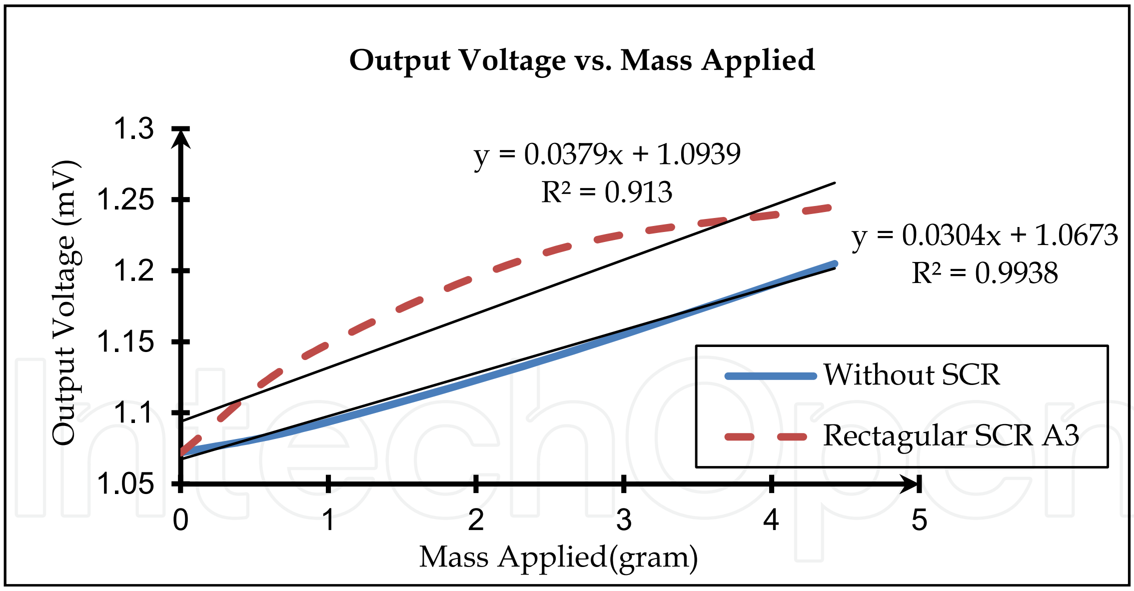

Figure 29. Output voltage when varying mass applied for piezoresistive MEMS cantilever without SCR and with rectangular SCR A3.

5. Conclusions

The piezoresistive MEMS cantilever has been design, analysed and fabricated in this research. FEA analysis results show that rectangular SCR design has the highest stress developed during force applied compared to other designs. The piezoresistive MEMS cantilever with rectangular SCR and without SCR were fabricated and characterised. Results show that the fabricated piezoresistive MEMS cantilever has successfully enhanced the sensitivity by 1.97 times compared to fabricated piezoresistive MEMS cantilever without SCR. The difference between FEA sensitivity analysis value and the fabricated device sensitivity value is 1.5%.

Author details

Sh Mohd Firdaus*
Faculty of Mechanical Engineering, University Technology MARA (UiTM), Penang, Malaysia

Husna Omar
Faculty of Applied Science, University Technology MARA (UiTM), Penang, Malaysia

Ishak Abd Azid
Faculty of Mechanical Engineering, University Science of Malaysia (USM), Penang, Malaysia

Acknowledgement

The authors wish to thank University Techology MARA, University Science of Malaysia and the Government of Malaysia for the offer of the e-science grant (Ref:6013205), fundamental research grant scheme (600-RMI/FRGS 5/3 (39/2012)) and Excellent Fund UiTM (600-RMI/ST/DANA 5/3/Dst (113/2011) that have enabled this research to be carried out.

6. References

Arik M, Zurn S.M, Yigit K.S and Bar-Cohen A, (1999). Design, Fabrication and Experimental-Numerical Study of PZT Sensors, University of Minnesota, MN 55455.

Arscott S., Legrand B., Buchaillot L. and Ashcroft A.E. (2007). A Silicon Beam-Based Microcantilever Nanoelectrosprayer. Sensors and Actuators B Vol.125, pp. 72–78.

Beeby S., Ensell G., Kraft M. and White N. (2004). MEMS Mechanical Sensors. Artech House,Canton Street, Norwood.

Behrens I., Doering L. and Peiner E. (2003). Piezoresistive Cantilever as Portable Micro Force Calibration Standard. Journal of Micromechanical Microengineering, Vol. 13, pp. 171-177.

Benham, P.P. Drawford, R.J. and Armstrong, C.G. (1996). *Mechanics of Engineering Materials.* Prentice Hall Ltd., UK

Bhatti M. A., Lee C. X., Lee Y. Z. and Ahmed N. A. (2007). Design and Finite Element Analysis of Piezoresistive Cantilever with Stress Concentration Holes. 2nd IEEE Conference on Industrial Electronics and Applications

Boylestad, R. L. (2003). Introductory Circuit Analysis. Pearson Pr entice Hall, Upper Saddle River, New Jersey.

Brugger J., Despont M., Rossel C., Rothuizen H., Vettiger P. and Willemin M. (1999). Microfabricated Ultrasensitive Piezoresistive Cantilevers for Torque Magnetometry. Sensors and Actuators A Vol.73, pp. 235-242.

* Corresponding Author

Calleja M., Nordstrom M., Alvarez M., Tamayo J., Lechuga L.M. and Boisen A. (2005). Highly Sensitive Polymer-based Cantilever-Sensors for DNA Detection, Journal of Ultramicroscopy, Vol. 105, pp. 215-222.

ChatrathiI K., Packirisamy M., Stiharu I., Nerguizian V. (2006). Effect of Curvature on Dynamic Behavior of Cantilever. MEMS IEEE ISIE 2006, Quebec, Canada.

Chollet Frank and Liu Haobing. (2007). A short introduction to MEMS. Micromachines Centre, School of MAE, Nanyang Technological University, Singapore.

Chivukula V., Wang M, Ji Hai-Feng, Abdul Khaliq, Ji Fang, Kody Varahramyan, (2006). Simulation of SiO_2 based Piezoresistive Microcantilevers. Sensors and Actuators A, Vol. 125, pp. 526-533.

Chu Duc T., Creemer J.F. and Sarro Pasqualina M., (2007), "Piezoresistive Cantilever Beam for Force Sensing in Two Dimensions", IEEE Sensors Journal, Vol.7, No.1.

Chu Duc T., Creemer J.F. and Sarro Pasqualina M. (2006). Lateral Nano-Newton Force-Sensing Piezoresistive Cantilever for Microparticle Handling. Journal of Micromechanical Microengineering, Vol. 16, pp. 102-106.

Cook Nigel P. (1996). Practical Electricity. Pearson Prentice Hall, Upper Saddle River, New Jersey.

Don Klaitabtim and Adisorn Tuantranon, (2005). Design Consideration and Finite Element Modeling of MEMS Cantilever for Nano-Biosensor Applications. Proceedings of 2005 5th IEEE Conference on Nanotechnology Nagoya, Japan.

Eklund E. J. and Shkel A. M., (2007). Single-mask fabrication of high-G piezoresistive accelerometers with extended temperature range. Journal of Micromechanics and Microengineering. Vol. 17 (4), pp. 730-736

Fan Z., Chen J., Zou J., Bullen D. 1, Liu C. and Delcomyn F. (2002). Design and Fabrication of Artificial Lateral Line Flow Sensors. Journal of Micromechanical Microengineering. Vol. 12, pp. 655–661.

Fuller L.F. Microelectronic Engineering Department of Rochester, Institute of Technology (2007).Available from World Wide Web: http: www.rit.edu/~iffee/[Accessed 8 January 2008].

Gel M., and Shimoyama I.(2004). Force Sensing Submicrometer Thick Cantilever with Ultra-Thin Piezoresistors by Rapid Thermal Diffusion. Journal of Micromechanical Microengineering, Vol.14, pp. 423-428.

Guillermo V. T. L. (2006). Development of Cantilever for Biomolecular Measurement. Ph.D. Dissertation, Universitat Autonoma de Barcelona, Barcelona, Spain.

Cheng F.H., (1998). Statics and Strength of Materials. Mc Graw-Hill International, Civil Engineering Series.

He J. H. and Li Y. F. (2006). High Sensitivity Piezoresistive Cantilever Sensor for Biomolecular Detection. Journal of Physic: Conference Series, Vol. 34, pp. 429-435.

Hsu, Tai-Ran. (2002). MEMS & Microsystems – Design and Manufacture. McGraw Hill International Series, Singapore Madou M. (1997). Fundamental of Microfabrication. CRC Press, Boca Raton.

Jiang Y.G., Ono T. and Eshashi M. (2008). Fabrication of Piezoresistive Nanocantilevers for Ultra-Sensitive Force Detection. Measurement Science and Technology, Vol.19, 84011

Joshi B.P., Joshi Aditee, and Gangal S.A. (2007), Performance Improvisation of Cantilever type Silicon Micro Acceleration Sensors using Stress Concentration Regions Technique, Defense Science Journal, Vol. 57, pp. 271-279.

Lee H. J., Young S. C., Lee Y.P., Jeong K.H. and Kim H.Y. (2007). Deflection of Microcantilever by Growing Vapor Bubble. Sensors and Actuators A, Vol. 136, pp. 717–722.

Li M, Tang H.X. and Roukes M.L.(2007). Ultra-Sensitive NEMS-based Cantilevers for Sensing, Scanned Probe and Very High-Frequency Applications. Nature Nanotechnology, Vol. 2, pp. 114-120.

Liu Chang. (2006). Foundation of MEMS. Illinois ECE series, Pearson Education, Upper Saddle River, New Jersey.

Loui A., Goericke F.T., Ratto T.V., Lee J., Hart B.R. and King W.P. (2008). The Effect of Piezoresistive Microcantilever Geometry on Cantilever Sensitivity during Surface Stress Chemical Sensing. Sensors and Actuators A, Vol. 147, pp. 516-521.

Park D. S., Yun D.J., Cho M. W. and Shin B.C. (2007). An Experimental Study on the Fabrication of Glass-based Acceleration Sensor Body Using Micro Powder Blasting Method. Sensors 2007, Vol. 7, pp. 697-707.

Peiner E., Doering L. and Balke M. (2008). Silicon Cantilever Sensor forMicro/Nanoscale Dimension and Force Metrology. Technical Paper of Microsystems Technology, Vol. 14, pp. 441-451

Pramanik C., Saha H. and Gangopadhyay U., (2006). Design Optimization of a High Performance Silicon MEMS Piezoresistive Pressure Sensor for Biomedical Applications, Journal of Micromech. Microeng. Vol. 16, pp. 2060-2066.

Rosmazuin A.R., Badariah B., and Burhanuddin Y.M., (2008), Design and Analysis of MEMS Piezoresistive SiO_2 Cantilever-based Sensor with Stress Concentration Region for Biosensing Applications, ICSE 2008 Proceeding, Johor Bahru, Malaysia.

Saya D., Belaubre P., Mathieu F., Lagrange D., Pourciel J.B., Bergaud C.(2005). Si-Piezoresistive Microcantilever for Highly Integrated Parallel Force Detection Applications. Sensors and Actuators A, Vol. 123-124, pp. 23-29.

Sone H. , Okano H. and Sumio H. (2004). Picogram Mass Sensor using Piezoresistive Cantilever for Biosensor. Japanese Journal of Applied Physics, Vol. 43(7b), pp. 4663–4666.

Streetman B. G. and Banerjee S. K. (2006). Solid State Electronic Devices 6thEdition. Pearson Prentice Hall, Upper Saddle River, New Jersey

Su Y., Evans A.G.R. and Brunnshweiler.(1996). Micromachine Silicon Cantilever Paddles with Piezoresistive Readout for Flow Sensing. Journal Micromechanical Microengineering, Vol.6, pp. 69-72.

Thundat T., Chen G.Y., Warmack R.J., Allison D.P. and Wachter E.A. (1995). Vapor Detection using Resonating Microcantilever. Anal. Chemical. Vol. 67, pp. 519-521.

Vashist K. S. (2007). A Review of Microcantilever for Sensing Applications. Journal of Nanotechnology Online, Vol. 3, June 2007.

Yoo K.A., Kim J.H., Nahm B.H., Kang C.J. and Kim Y.S. (2007) Fabrication and Characteristics of Microcantilever-based Biosensor for Detection of the Protein-Ligand Binding, Journal of Physics: Conference Series Vol. 61, pp. 1308–1311.

Yu X., Zhang H., Li X., Li T. and Zhang D. (2007). Design of High-Sensitivity Cantilever and Its Monolithic Integration with CMOS Circuits, IEEE Sensor Journal, Vol. 7, pp. 489-494.